



Effects of velocity, thermal and solutal slip boundary conditions on the flow and heat transfer of nanofluids past a linear stretching sheet with prescribed constant wall temperature

M. Subhas Abel* and N. Rajesh Singh Shambajee**

*Professor department of mathematics Gulbarga University, Kalaburagi Karnataka, India

**Research scholar department of mathematics Gulbarga University, Kalaburagi India

(Corresponding author: M. Subhas Abel)

(Received 28 September, 2016 Accepted 29 October, 2016)

(Published by Research Trend, Website: www.researchtrend.net)

ABSTRACT: This paper considers the problem of steady laminar two dimensional boundary layer flow and heat transfer of nanofluids past a linear stretching sheet. The governing boundary value problem, consisting of equations of motion and heat transfer for a nanofluid flow past an linear stretching sheet, with their respective boundary conditions are considered for investigation. This boundary value problem consisting of nonlinear partial differential equations are transformed into nonlinear ordinary differential equations using suitable similarity transformation and are solved numerically solved by using fourth order Runge-Kutta method, along with shooting technique. The solution mainly depends on Prandtl number Pr , Lewis number Le , Brownian motion parameter N_b and thermophoresis parameter N_t , velocity slip parameter A , thermal slip parameter B and solutal slip parameter C . The variation of the local Nusselt number and local Sherwood number with N_b and N_t for various values of Pr and Le is presented in tabular and graphical forms. It is found that for $A=B=C=0$ (No slip boundary condition) local nusselt number decreases and local Sherwood number increases as N_t parameter increases. Further it is observed that as the velocity slip parameter A increases, local Nusselt number decreases and local Sherwood number decreases. As the thermal slip parameter B increases local nusselt number decreases and local sherwood number increases. As the solutal slip parameter C increases local nusselt number increases and local Sherwood number decreases.

Keywords: Nanofluid, Stretching sheet, Slip boundary conditions, Brownian motion, Thermophoresis, Heat transfer, Similarity solution, boundary layer flow, linear stretching sheet.

I. INTRODUCTION

The study of laminar boundary layer flow over a stretching sheet has received substantial notice in the past owing to its applications in the industries, for example, materials contrived by extrusion process and the heat treated materials drifting amid a feed roll and the wind-up roll or on conveyor belt possess the character of a poignant continuous surface have promising applications in a numeral of technological processes as well as production of polymer films or thin sheets. Few of these applications are materials manufactured by polymer extrusion, drawing of copper wires, continuous stretching of plastic films, artificial fibres, hot rolling, wire drawing, glass fibre, metal extrusion and metal spinning etc. The boundary layer flow and heat transfer owing to nanofluids over a stretching sheet are thrust areas of current research. Such investigations locate applications over a broad spectrum of science and engineering disciplines. An imperative aspect of boundary layer flow of a nanofluid over a stretching sheet is the heat transfer characteristics. It is vital to comprehend the heat transfer description of the stretching sheet so that the

completed product meets the required quality. This is owing to the aspect that the superiority of a final product chiefly depends on the rate of heat transfer and the stretching rate.

Kuznestov and Nield [1] have deliberated the natural convective boundary-layer flow of a nanofluid past a vertical plate analytically. They worn a model in which Brownian motion and thermophoresis property be taken into account. Furthermore, Khan and Pop [2] use the same model to learn the boundary layer flow of a nanofluid past a stretching sheet with a constant surface temperature. Very recently Ibrahim and Shanker [3] have studied the boundary-layer flow and heat transfer of nanofluid over a vertical plate taking into account the convective surface boundary condition. Recently, Haddad *et al.* [4] experimentally investigated natural convection in nanofluid by considering the function of thermophoresis and Brownian motion in heat transfer enhancement. They indicated that neglecting the role of Brownian motion and thermophoresis depreciate the heat transfer and this weakening elevates when the volume fraction of a nanoparticles increases.

Likewise Bachok *et al.* [5] numerically studied steady boundary layer flow of a nanofluid over a moving semi-infinite plate in a regular free stream. Further, Makinde and Aziz [6] conducted a numerical study of boundary layer flow of a nanofluid past a stretching sheet with convective boundary condition. Also, Vajravelu *et al.* [7] discussed the convective heat transfer of a nanofluid flow over a stretching surface using Ag-water or Cu-water nanofluid.

A familiar feature of all the above studies considered is the no-slip boundary condition. But, there may be natural circumstances where no-slip boundary condition may not be pertinent. In such situation, it may be imperative to consider slip boundary condition. Fluids like water and gaseous (air) viscosity is very small (negligible) but fluid such as oil, glycerine, paints, molecule, printer ink possess large viscosity, where there exists a difference in relative tangential velocity i.e. there is a slip in the boundary. On the other hand the existence of intermolecular pull makes the fluid to stick to a solid wall and this gives rise to the shearing stresses and there will be no-slip from the boundary. The no-slip boundary condition is known as the main manifestation of the Navier-Stoke's theory of fluid dynamics. But there are situations wherein such condition is not appropriate. Especially no-slip condition is inadequate for most non-Newtonian liquids and nanofluids, as some polymer melt often shows microscopic wall slip and that in general is governed by a non-linear and monotone relation between the slip velocity and the traction. The liquids exhibiting boundary slip find applications in technological problems such as polishing of artificial heart valves and internal cavities.

The slip flow boundary condition was first introduced by C.L.M.H. Navier more than a century ago. The earlier studies that take into account the slip boundary condition over a stretching sheet were conducted by Andersson [8]. He obtained a closed form solution of a full Navier-Stoke's equations for a magnetohydrodynamics flow over a stretching sheet. Following Andersson, Wang [9] set up the closed form similarity solution of a full Navier-Stoke's equations for the flow due to a stretching sheet with partial slip. Furthermore, Wang [10] investigated stagnation slip flow and heat transfer on a moving plate. Similarly, Fang *et al.* [11] studied MHD slip viscous flow over a stretching sheet analytically. P. Donald Ariel [12] investigated the steady, laminar, axisymmetric flow of a Newtonian fluid due to a stretching sheet when there is a partial slip of the fluid past the sheet. He applied the HPM method to obtain the solution of B.V.P. T. Hayat, T. Javed, Z. Abbas [13] examined the effect of slip flow and heat transfer of a second grade fluid past a stretching sheet through a porous space. He applied the H.A.M. method to

solve the problem. M. Turkyilmazoglu [14] studied the heat and mass transfer characteristics of the M.H.D. viscous flow over a permeable stretching surface considering both the hydrodynamic and thermal slip boundary conditions. He solved the problem by using the confluent Hypergeometric functions. Abdul Aziz [15] investigated numerically the hydrodynamic and thermal characteristics of the boundary layer flow over a flat plate with slip and constant heat flux. Bikash Sahoo [16] studied the effects of partial slip on the steady flow and heat transfer of an incompressible, thermodynamically compatible third grade fluid past a stretching sheet. An effective second order numerical scheme has been used to solve the governing equations with inadequate boundary conditions. M. Turkyilmazoglu [17] examined the M.H.D. boundary layer problem for momentum and heat transfer with dissipative energy, thermal radiation and internal heat source/sink in conducting fluid flow over a porous stretching sheet under the condition of velocity slip on the wall. He solved it analytically. M.M. Rahman [18] studied the heat transfer process in a two-dimensional steady viscous incompressible hydro- magnetic convective flow of an electrically conducting fluid over a flat plate with partial slip at the surface of the boundary subjected to the conducting fluid over a flat plate with partial slip at the surface of the boundary subjected to the convective surface heat flux at the boundary. He solved numerically the problem by using the Nachtsheim-Swigert iteration procedure. Bikash Sahoo [19,20] studied the effects of partial slip on the steady flow of a incompressible, electrically conducting third grade non-Newtonian fluid due to stretching sheet. He solved it numerically. Dileep Singh Chauhan and Amala Olkha [21] examined the boundary layer slip flow of a second-grade fluid in a porous medium past a stretching sheet and heat transfer characteristics with power-law surface temperature or heat flux. He solved it by confluent Kummer's Hyper-geometric function.

Recently, Aminreza Noghrehabadi, Rashid Pourrajab, Mohammad Ghalambaz [22] investigated the effect of partial slip (momentum or velocity slip) boundary condition on the flow and heat transfer of nanofluids past stretching sheet prescribed constant wall temperature. This problem is solved by using Runge-Kutta-Fehlberg scheme with shooting method. They indicated that the reduced Nusselt number and Sherwood number are strongly influenced by the velocity slip parameter. Wubshet Ibrahim, Bandari Shankar [23] investigated the boundary layer and heat transfer over a permeable stretching sheet due to a nano fluid with the effect of magnetic field, slip boundary condition and thermal radiation. He solved it by fourth order Runge-Kutta method with shooting technique.

Thus motivated by the above mentioned investigations and applications of linear stretching sheet, we investigated the effect of partial slip boundary conditions on the steady laminar two dimensional boundary layer flows and heat transfer of nanofluids past a linear stretching sheet. We investigated that the skin friction coefficient ($-f'(0)$),

reduced Nusselt number ($-\theta'(0)$) and reduced Sherwood number ($-\phi'(0)$) are strongly influenced by the velocity slip parameter A, thermal slip parameter B and solutal slip parameter C.

Nomenclature	
A	velocity (or momentum) slip parameter
B	thermal slip parameter
C	solutal(or concentration) slip parameter
a,b,c	constants
C_f	skin friction coefficient
u_w	is the velocity of the stretching sheet
C_w	is nanoparticles volume fraction at the stretching surface
C_∞	ambient nanoparticles volume fraction
D_B	Brownian diffusion coefficient
D_T	thermophoresis diffusion coefficient
f	dimensionless stream function
κ	thermal conductivity
Pr	Prandtl number
Le	Lewis number
Nb	Brownian motion parameter
Nt	thermophoresis
Nu_x	local Nusselt number
Sh_x	local Sherwood number
Re_x	local Reynolds number
T_w	uniform temperature over the surface of the sheet
T_∞	ambient temperature or is the temperature far away from the sheet
T	temperature of the fluid inside the boundary layer
u,v	velocity component along x and y-direction
p	is the fluid pressure
Greek symbols	
η	dimensionless similarity variable
μ	dynamic viscosity of the fluid
ν	kinematic viscosity of the fluid
ϕ	dimensionless concentration function
ρ_f	density of the fluid
$(ap)_f$	heat capacity of the fluid
$(ap)_p$	effective heat capacity of a nano fluid
Ψ	stream function
α	thermal diffusivity
θ	dimensionless temperature
τ	parameter defined by $(ap)_p / (ap)_f$
Subscripts	
∞	condition at the free stream
w	condition of the surface

II. MATHEMATICAL FORMULATION

Consider the two-dimensional boundary layer flow of a nanofluid past a stretching surface in which the flow is viscous, incompressible and steady state. The velocity of surface is linear and it can be represented as $u_w(x) = ax$. Here “a” is constant and x is the coordinate measured along the stretching surface as shown in Fig 1.



Fig 1 Physical model and co-ordinate system

The nanofluid flows at $y = 0$, where y is the co-ordinate measured normal to the stretching surface. A steady uniform stress leading to equal and

opposite forces (i.e. two equal and opposite forces) are applied along the x-axis, so that the sheet is stretched keeping the origin fixed. The fluid adheres to the sheet partially and the motion of the nanofluid exhibits the slip condition. It is assumed that at the stretching surface, the temperature T and the nanoparticles fraction C take constant values T_w and C_w respectively. When y attains infinity, the ambient values of temperature T and nanoparticles fraction C are denoted by T_∞ and C_∞ respectively. It is assumed that the base fluid and the suspended nanoparticles are in thermal equilibrium. It is chosen that the co-ordinate system x-axis is along stretching sheet and y-axis is normal to the sheet. In the laminar sub layer near the wall, Brownian diffusion and thermophoresis are important for nanoparticles of any material and size for nanofluid.

The basic steady conservation of mass, momentum, thermal energy and nanoparticles equations for nanofluids can be written in Cartesian co-ordinates x and y as, see Kuznetsov and Nield [24]. The flow and heat transfer characteristics under the boundary layer approximations are governed by the following equations.

$$\frac{\partial u}{\partial x} + \frac{\partial v}{\partial y} = 0 \tag{1}$$

$$u \frac{\partial u}{\partial x} + v \frac{\partial u}{\partial y} = \nu \left(\frac{\partial^2 u}{\partial y^2} \right) \tag{2}$$

$$u \frac{\partial T}{\partial x} + v \frac{\partial T}{\partial y} = \alpha \left(\frac{\partial^2 T}{\partial y^2} \right) + \tau \left\{ D_b \left(\frac{\partial C}{\partial y} \frac{\partial T}{\partial y} \right) + \left(\frac{D_T}{T_\infty} \right) \left[\left(\frac{\partial T}{\partial y} \right)^2 \right] \right\} \tag{3}$$

$$u \frac{\partial C}{\partial x} + v \frac{\partial C}{\partial y} = D_b \left(\frac{\partial^2 C}{\partial y^2} \right) + \left(\frac{D_T}{T_\infty} \right) \left(\frac{\partial^2 T}{\partial y^2} \right) \tag{4}$$

The boundary conditions are

$$v=0, u=u_w + L_1 \frac{\partial u}{\partial y}, T=T_w + L_2 \frac{\partial T}{\partial y}, C=C_w + L_3 \frac{\partial C}{\partial y} \text{ at } y=0 \tag{5}$$

$$u=v=0, T=T_\infty, C=C_\infty \text{ as } y \rightarrow \infty \tag{6}$$

Where u and v are the velocity components along x and y axis respectively. $\nu = \mu/\rho_f$ is the kinematic viscosity, $\alpha = \kappa/(c\rho)_f$ is the thermal diffusivity, D_b is the Brownian diffusion coefficient, D_T is the thermophoresis diffusion coefficient and $\tau = (\rho a)_p / (\rho a)_f$ is the ratio between the effective heat capacity of the nanoparticles material and heat capacity of the nano fluid. T is the temperature inside the boundary layer, T_∞ is the temperature far away from the sheet. $u_w(x) = ax$ is the stretching velocity of the sheet, $T_w = T_\infty + b(x/l)^2$ is the temperature of stretching surface and $C_w = C_\infty + c(x/l)^2$ is nanoparticles volume fraction at the stretching surface. L_1 is the velocity slip factor, L_2 is thermal slip factor and L_3 is concentration slip factor. Note that when $L_1 = L_2 = L_3 = 0$ the no-slip condition is recovered, l is the reference length of a sheet and the above boundary condition is valid when $x \leq l$ which occurs very near to the slit.

We are interested in similarity solution of the above boundary value problem, therefore we introduce the following similarity transformations (dimensionless quantities).

$$\left. \begin{aligned} \eta &= \left(\frac{a}{\nu} \right)^{1/2} y, \quad \psi = (a\nu)^{1/2} x f(\eta), \quad \theta(\eta) = \frac{T - T_\infty}{T_w - T_\infty}, \\ \phi(\eta) &= \frac{C - C_\infty}{C_w - C_\infty}, \quad u = ax f'(\eta), \quad v = - \left(\frac{a\nu}{\rho} \right)^{1/2} f(\eta) \end{aligned} \right\} \tag{7}$$

In eqn(7), f denotes the non-dimensional stream function, the prime denotes differentiation with respect to η and the stream function ψ is defined in the usual way as $u = \partial\psi/\partial y$, $v = -\partial\psi/\partial x$. Making use of transformations (7) in (1), we can realize incompressibility condition (i.e. continuity equation) is identically satisfied and the governing eqns (2) – (4) takes the form of non-linear ordinary differential equations:

$$f''' + f f'' - f'^2 = 0 \tag{8}$$

$$\theta' + Pr f \theta' + Pr Nb \phi' \theta' + Pr Nt \theta'' = 0 \tag{9}$$

$$\phi'' + Le f \phi' + \frac{Nt}{Nb} \theta' = 0 \tag{10}$$

with the boundary conditions:

$$\left. \begin{aligned} f(0) &= 0, \quad f'(0) = 1 + Af''(0), \quad \theta(0) = 1 + B\theta'(0), \\ \phi(0) &= 1 + C\phi'(0) \text{ at } \eta = 0 \\ f'(\infty) &= 0, \quad \theta(\infty) = 0, \quad \phi(\infty) = 0 \text{ as } \eta \rightarrow \infty \end{aligned} \right\} \tag{11}$$

Where f , θ and ϕ are dimensionless velocity, temperature and nanoparticles concentration, respectively. η is the similarity variable, the prime denote differentiation with respect to η and the governing parameters appearing in eqs (8) to (11) are defined by

$$\left. \begin{aligned} Pr &= \frac{\nu}{\alpha} \rightarrow \text{Prandtl number}; \quad Nb = \frac{(\rho c)_p D_b (\theta_w - \phi_w)}{(\rho c)_f \nu} \rightarrow \text{Brownian motion parameter} \\ Le &= \frac{\nu}{D_b} \rightarrow \text{Lewis number}; \quad Nt = \frac{(\rho c)_p D_T (T_w - T_\infty)}{(\rho c)_f T_\infty \nu} \rightarrow \text{Thermophoresis parameter} \\ A &= L_1 \sqrt{\frac{a}{\nu}} \rightarrow \text{Velocity slip parameter}; \quad B = L_2 \sqrt{\frac{a}{\nu}} \rightarrow \text{Thermal slip parameter} \\ C &= L_3 \sqrt{\frac{a}{\nu}} \rightarrow \text{Solutal slip parameter} \end{aligned} \right\} \tag{12}$$

It is important to note that this boundary value problem reduces to the classical problem of flow and heat and mass transfer due to a stretching surface in a viscous fluid when Nb and Nt are zero in eqs.(9)-(10) (i.e. The boundary value problem for ϕ then becomes ill-posed and is of no physical significance).

It is also noted that when $A=B=C=0$ (i.e. the no-slip condition) in eqn. (11), then we get usual boundary conditions $f'(0) = 1$, $\theta(0) = 1$ and $\phi(0) = 1$ at $\eta = 0$. Further, when $A=B=C=0$, the fluid sticks to the boundary and when $A, B, C \rightarrow \infty$, the fluid slips past the boundary without any resistance. The significant corporeal quantities of interest in this problem are local Skin friction coefficient C_f , the local Nusselt number Nu_x and the local Sherwood number Sh_x are defined as:

$$C_f = \frac{\tau_w}{\rho u_w^2}, \quad Nu_x = \frac{x q_w}{k(T_w - T_\infty)}, \quad Sh_x = \frac{x q_m}{D_B(C_w - C_\infty)} \quad (13)$$

Where wall shear stress τ_w , wall heat flux q_w , mass flux q_m are given by:

$$\tau_w = \rho \nu \left(\frac{\partial u}{\partial y} \right)_{y=0}, \quad q_w = -k \left(\frac{\partial T}{\partial y} \right)_{y=0}, \quad q_m = -D_B \left(\frac{\partial \phi}{\partial y} \right)_{y=0} \quad (14)$$

By solving eqs.(13) using eqs.(7),(14).We get

$$C_f \sqrt{Re_x} = -f''(0), \quad \frac{Nu_x}{\sqrt{Re_x}} = -\theta'(0) = Nur, \quad \frac{Sh_x}{\sqrt{Re_x}} = -\phi'(0) = Shr \quad (15)$$

Where $C_f, Nu_x (Nur), Sh_x (Shr), Re_x$ are the skin friction, local Nusselt number and local Sherwood number respectively.

III. NUMERICAL SOLUTION.

An well-organized fourth order Runge-Kutta method along with Shooting technique has been engaged to study the flow model of the above coupled non-linear ordinary differential equations (8) - (10) for different values of governing parameters viz. Prandtl number Pr , Lewis parameter Le , Brownian motion parameter Nb , thermophoresis parameter Nt , velocity slip parameter A , thermal slip parameter B and solutal slip parameter C . The non-linear differential equations are first decomposed into a system of first order differential equations. The coupled ordinary differential eqs.(8)-(10) are third order in f and second order in θ and ϕ which have been reduced to a system of seven simultaneous equations for seven unknowns. In order to numerically solve this system of equations using Runge-Kutta method, the solution requires seven initial conditions but two initial conditions in f and one initial condition in each of θ and ϕ are known. However, the values of f, θ and ϕ are known at $\eta \rightarrow \infty$. These end conditions are utilized to produce unknown initial conditions at $\eta = 0$ by Shooting technique. The most important step of this scheme is to choose the appropriate finite

value of η_∞ . Thus to estimate the value of η_∞ , we start with some initial guess value and solve the boundary value problem consisting of Eqs. (8)-(10) to obtain $f''(0), \theta'(0)$ and $\phi'(0)$. The solution process is repeated with another larger value of η_∞ until two successive values of $f''(0), \theta'(0)$ and $\phi'(0)$ differ only after desired significant digit. The last value η_∞ is taken as the finite value of the limit η_∞ for the particular set of physical parameters for determining velocity, temperature, and concentration, respectively are $f(0), \theta(0)$ and $\phi(0)$ in the boundary layer. After getting all the initial conditions we solve this system of simultaneous equations using fourth order Runge-Kutta integration scheme. The value of η_∞ is selected to vary from 5 to 20 depending on the physical parameters governing the flow so that no numerical oscillation would occur.

In the present analysis, the boundary value problem is first converted into an initial value problem (IVP). Then the IVP is solved by appropriately guessing the missing initial value using the shooting method for several sets of parameters. The step size $h=0.1$ is used for the computational purpose. The error tolerance of 10^{-6} is also being used. The results obtained are presented through tables and graphs, and the main features of the problems are discussed and analyzed.

IV. RESULTS AND DISCUSSION.

The numerical solutions are obtained for velocity, temperature and concentration profiles for different values of governing parameters. The obtained results are displayed through graphs **Figs.2-12** for velocity, temperature and concentration profiles, respectively.

Fig 2(a) shows the effect of dimensionless similarity functions $f(\eta), f'(\eta), f''(\eta)$ for different values of velocity slip parameter A . As the value of velocity slip parameter A increases, the velocity normal to the sheet $f(\eta)$, mainstream velocity profiles $f'(\eta)$ decreases and magnitude of wall shear stress $f''(\eta)$ increases.

Fig 2(b) indicates the velocity slip parameter A increases in magnitude, permitting more fluid to slip past the sheet, the skin-friction coefficient $-f''(0)$ decreases in magnitude and approaches to zero for higher values of the slip parameter, i.e. the flow behaves as though it were inviscid. This implies that the frictional resistance between the fluid and the surface of the sheet is eliminated and the stretching of sheet does no longer impose any motion on the fluid and the flow behaves as though it were inviscid.

This observation is agreement with the study reported by Andersson [8] for a non-magnetic viscous fluid. Therefore, the skin-friction coefficient decreases as the values of velocity slip parameter (A) increases

Fig 3. shows the effect of different values of velocity slip parameter A on dimensionless velocity profiles $f'(\eta)$. From the figure it is clear that as the value of velocity slip parameter A increases the velocity profile $f'(\eta)$ decreases. Further it is observed that for velocity slip parameter $A=0$ (i.e. no-slip condition) the graph approaches unity, hence it satisfies usual boundary condition $f'(0) = 1$.

Fig 4. shows the effect of different values of velocity slip parameter A on temperature profiles $\theta(\eta)$. From the figure one can see that as the value of velocity slip parameter ($A = 0, 0.5, 1, 2, 5$) increases the temperature profiles also increases, which results in thickening of the thermal boundary layer.

Fig 5. shows the variation of temperature with respect to thermal slip parameter B . The graph reveals that the wall temperature $\theta(\eta)$ and the thermal boundary layer thickness decreases when the values of B increases.

Fig 6. shows the effect of different value of Prandtl number Pr on the temperature profiles. From the graph it is noticed that temperature decreases with the increasing value of Prandtl number ($Pr=1, 2, 3, 4$) because thermal boundary layer thickness decreases due to increase in Pr . In short, an increase in the Prandtl number means slow rate of thermal diffusion. The graph also shows that as the value of Prandtl number Pr increase, the wall temperature decreases. The effect of Prandtl number on a nanofluid is similar to what has already been observed in common fluids qualitatively but they are different quantitatively. Therefore, these properties are inherited by nanofluids.

Fig 7. shows the influence of the change of Brownian motion parameter Nb and thermophoresis parameter Nt on the temperature profile when ($Nt=Nb$). It is noticed that as the thermophoresis parameter Nt and brownian motion parameter Nb increases the thermal boundary layer thickness increases.

Fig 8. shows the variations of concentration profile for different values of velocity slip parameter A . It is noticed that the concentration profile increases as the value of velocity slip parameter $A=(0, 0.5, 1, 2, 5)$ increases. That means concentration profile is directly proportional to velocity slip parameter A .

Fig 9. Illustrates the variation of concentration profile with respect to concentration or solutal slip parameter C . As it can be seen from the graph, as the values of solutal slip parameter $C=(0.0, 0.5, 1, 2, 5)$ increases the concentration profile decreases, which results in thinning of concentration boundary layer.

Fig 10. Shows the variation of concentration profiles for different values of Lewis number Le .

It is noticed that concentration profile decreases with the increasing value of Lewis number ($Le=1, 2, 5, 8, 10$). Moreover, the concentration at the surface of a sheet decreases as the values of Le increase. From the plots it is evident that large values of Lewis number results in thinning of concentration boundary layer of nanofluid.

Fig 11. reveals variation of concentration profiles in response to a change in thermophoresis parameter Nt . The influence of thermophoresis parameter on concentration profile graph is monotonic, i.e. as the values of Nt increase, the concentration boundary layer thickness is also increasing. Moreover, it is possible to recognize from the graph that the magnitude of concentration gradient on the surface of a sheet decrease as the values of Nt increase.

Fig 12. reveals the variation of concentration profile in response to a change in Brownian motion parameter Nb . As the values of Brownian motion parameter ($Nb=0.5, 1.5, 4$) increases, the concentration boundary layer thickness is decreasing. Furthermore, the magnitude of concentration gradient on the surface of a sheet increases as the values of Nb increase.

Finally, a comparison with published papers available in the literature has been done in order to check the accuracy of the present results. From the table 1, the skin friction coefficient $-f''(0)$ decreases as the velocity slip parameter A increases. It is interesting to find that as the velocity slip parameter A increases in magnitude, permitting more fluid to slip past the sheet, the skin-friction coefficient decreases in magnitude and approaches to zero for higher values of the slip parameter, i.e. the flow behaves as though it were inviscid. The numerical values of skin friction coefficient $-f''(0)$ in this paper are in excellent agreement with the result published in Anderson [8], Hayat et al. [25] and Wubshet Ibrahim [23].

From table 2 compares results for the local Nusselt number $-\theta'(0)$ and local Sherwood number $-\phi'(0)$ when $Le=Pr=10$ and $A=B=C=0$ (no slip condition) obtained in the present work with those reported by Khan and Pop [2] and Aminreza [22]. Consider that the zero value of slip factor simulates the stretching model used in the work of Khan and Pop [2] and Aminreza [22]. Table 3 shows that the present results are in good agreement with the results reported by Khan and Pop [2] and Aminreza [22].

From Tables 3, 4, & 5 shows the variation of the local Nusselt number $-\theta'(0)$ and local Sherwood number $-\phi'(0)$ respectively for different values of Nb, Nt, A, B and C when $Pr=10, Le=10$. In tables 2, 3, 4, and 5 we observe for $A=B=C=0$ (No slip boundary condition) nusselt number $-\theta'(0)$ decreases and Sherwood number $-\phi'(0)$ increases as Nt parameter is increased.

Table 3: As the slip parameter A increases Nusselt number decreases and Sherwood number decreases. As the Nt increases Nusselt number decreases and Sherwood number initially decreases afterwards increases as the value of Nt increases. Table 4: As the slip parameter B increases nusselt number decreases and sherwood number increases. As the Nt increases Nusselt number decreases and Sherwood number increases (B=0) and decrease for (B=1,2). Table 5: As the slip parameter C increases nusselt number increases and Sherwood number decreases. As the Nt increases nusselt number decreases and Sherwood number initially decreases but increases as the value of Nt increases.

Table 1: Comparison of skin friction coefficient $-f'(0)$ for different values of velocity slip parameter A.

A	Anders -on[8] [2002]	Hayat et - al.[25] [2011]	Wubshet Ibrahim[3] [2013]	Present results
0.0	1.0000	1.000000	1.0000	1.000000
0.1	0.8721	0.872082	0.8721	0.872083
0.2	0.7764	0.776377	0.7764	0.776378
0.5	0.5912	0.591195	0.5912	0.591196
2.0	0.2840	0.283981	0.2840	0.283980
5.0	0.1448	0.144841	0.1448	0.144840
10.0	0.0812	0.081249	0.0812	0.081248
20.0	0.0438	0.043782	0.0438	0.043785
50.0	0.0186	0.018634	0.0186	0.018636

Table 2: Comparison of results for the local Nusselt number $-\theta(0)$ and local Sherwood number $-\phi(0)$ when $Le=Pr=10$ and $A=B=C=0$ (no slip).

Nt	Nb	Khan & Pop [2] [2010]	Amurza Noghreha -bad[22] [2012]	Present result
		$-\theta(0)$	$-\theta(0)$	$-\theta(0)$
0.1	0.1	0.9524	0.9523768	0.952398
0.2		0.6932	0.6931743	0.693215
0.3		0.5201	0.5200790	0.520130
0.4		0.4026	0.4025808	0.402636
0.5		0.3211	0.3210543	0.321110
0.1	0.2	0.5056	0.5055814	0.505589
	0.3	0.2522	0.2521560	0.252444
	0.4	0.1194	0.1194059	0.119402
	0.5	0.0543	0.0542534	0.054253
0.2	0.3	---	---	0.181881
0.3		---	---	0.133775
0.4		---	---	0.104844
Nt	Nb	$-\phi(0)$	$-\phi(0)$	$-\phi(0)$
0.1	0.1	2.1294	2.1293938	2.129346
0.2		2.2740	2.2740215	2.273857
0.3		2.5286	2.5286382	2.528562
0.4		2.7952	2.7951701	2.794799
0.5		3.0351	3.0351425	3.034698
0.1	0.2	2.3819	2.3818706	2.381470
	0.3	2.4100	2.4100188	2.409953
	0.4	2.3997	2.3996502	2.399450
	0.5	2.3836	2.3835712	2.383571
0.2	0.3	---	---	2.514821
0.3		---	---	2.608559
0.4		---	---	2.751518

Table 3: Variation of local Nusselt number $-\theta(0)$ and local Sherwood number $-\phi(0)$ with Nb, Nt, A, B and C for Pr=10, Le=10.

Nt	Nb	A=B=C=0	A=0	A=1	A=2
		Khan and Pop[2] [2010]	B=C=0.5	B=C=0.5	B=C=0.5
		$-\theta(0)$	$-\theta(0)$	$-\theta(0)$	$-\theta(0)$
0.1	0.1	0.952398	0.833878	0.673747	0.601337
0.2		0.693215	0.729944	0.563843	0.496138
0.3		0.520130	0.614987	0.469074	0.408067
0.4		0.402636	0.523003	0.390850	0.337166
0.5		0.321110	0.445599	0.328184	0.281458
		$-\phi(0)$	$-\phi(0)$	$-\phi(0)$	$-\phi(0)$
0.1	0.1	2.129346	0.924238	0.803184	0.745320
0.2		2.273857	0.880439	0.780320	0.730982
0.3		2.528362	0.913120	0.825632	0.779544
0.4		2.794789	0.991242	0.905084	0.857160
0.5		3.039698	1.087907	0.994220	0.941270

Table 4: Variation of local Nusselt number $-\theta(0)$ local Sherwood number $-\phi(0)$ with Nb, Nt, A, B and C for Pr=10, Le=10.

Nt	Nb	A=B=C=0	B=0	B=1	B=2
		Khan and Pop[2] [2010]	A=C=0.5	A=C=0.5	A=C=0.5
		$-\theta(0)$	$-\theta(0)$	$-\theta(0)$	$-\theta(0)$
0.1	0.1	0.952398	1.016164	0.553389	0.363077
0.2		0.693215	0.747708	0.504821	0.350327
0.3		0.520130	0.576212	0.453543	0.335621
0.4		0.402636	0.459547	0.401871	0.318702
0.5		0.321110	0.376824	0.352578	0.299446
		$-\phi(0)$	$-\phi(0)$	$-\phi(0)$	$-\phi(0)$
0.1	0.1	2.129346	0.821794	0.874057	0.907301
0.2		2.273857	0.844327	0.822164	0.852447
0.3		2.528362	0.927475	0.825268	0.822325
0.4		2.794789	1.024498	0.873252	0.819584
0.5		3.039698	1.116684	0.902786	0.844684

Table 5: Variation of local Nusselt number $-\theta(0)$ and local Sherwood number $-\phi(0)$ with Nb, Nt, A, B and C for Pr=10, Le=10.

Nt	Nb	A=B=C=0	C=0	C=1	C=2
		Khan and Pop[2] [2010]	A=B=0.5	A=B=0.5	A=B=0.5
		$-\theta(0)$	$-\theta(0)$	$-\theta(0)$	$-\theta(0)$
0.1	0.1	0.952398	0.614059	0.769383	0.798057
0.2		0.693215	0.502341	0.653315	0.678561
0.3		0.520130	0.412373	0.552379	0.576078
0.4		0.402636	0.332870	0.467567	0.490540
0.5		0.321110	0.270709	0.398304	0.420418
		$-\phi(0)$	$-\phi(0)$	$-\phi(0)$	$-\phi(0)$
0.1	0.1	2.129346	1.792320	0.555161	0.328206
0.2		2.273857	1.827029	0.525570	0.306222
0.3		2.528362	1.985089	0.545804	0.315058
0.4		2.794789	2.198081	0.593044	0.340667
0.5		3.039698	2.414047	0.650331	0.372925

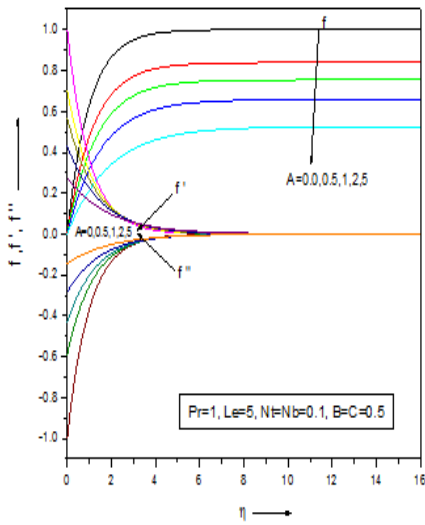


Fig 2(a). Effect of dimensionless similarity functions $f(\eta), f'(\eta), f''(\eta)$ for specified parameters.

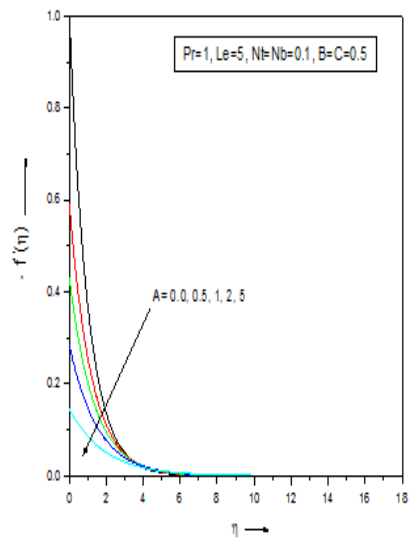


Fig 2(b). Effect of velocity slip parameter A on Skin friction coefficient $-f'(\eta)$ for specified parameter.

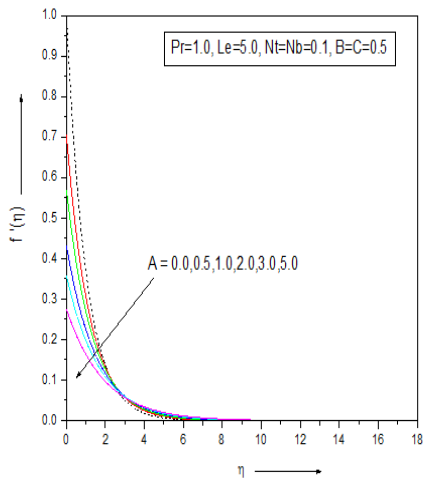


Fig 3. Effect of different values of velocity slip parameter A on dimensionless velocity profiles $f'(\eta)$

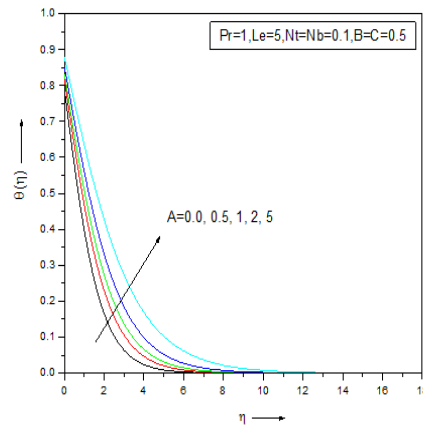


Fig 4. Effects of different values of velocity slip parameter A on temperature profiles

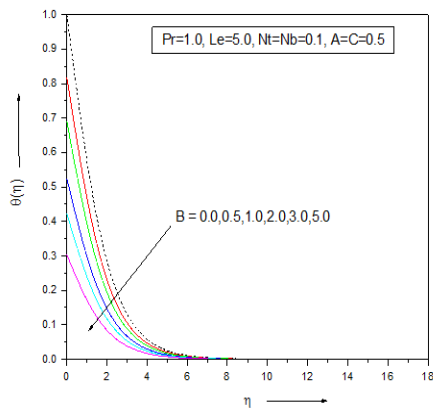


Fig 5. Effect of different values of thermal slip parameter B on the temperature profiles.

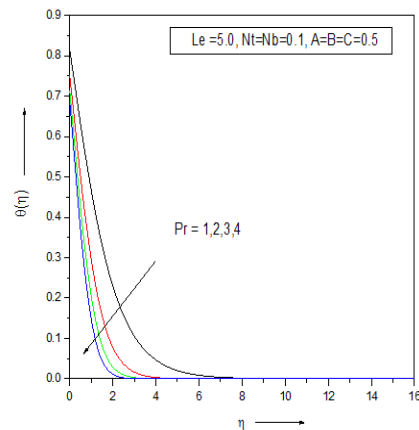


Fig 6. Effect of different value of Prandtl number Pr on the temperature profiles.

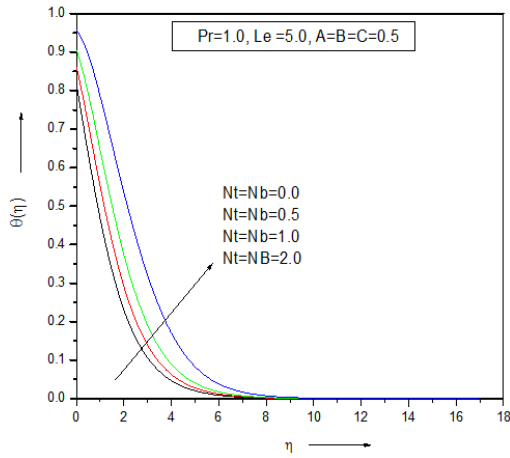


Fig 7. Effect of different values of Thermophoresis parameter Nt and Brownian motion parameter Nb on the temperature profiles.

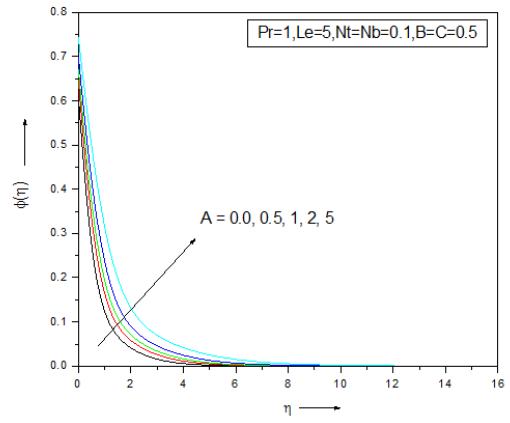


Fig 8. Effects of different values of velocity slip parameter A on the concentration profile.

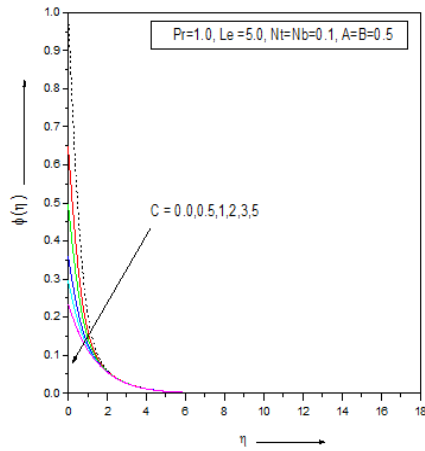


Fig 9. Effects of different values of solutal slip parameter C on the concentration profiles.

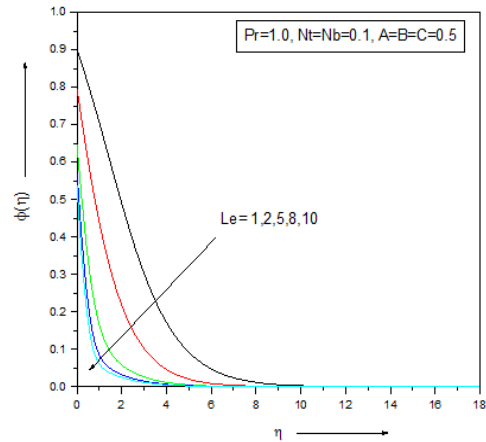


Fig 10. Effect of different values of Lewis number Le on the concentration profiles.

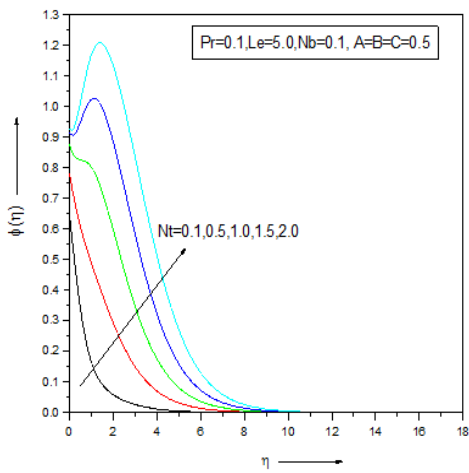


Fig 11. Effects of Thermophoresis parameter Nt on the concentration profiles.

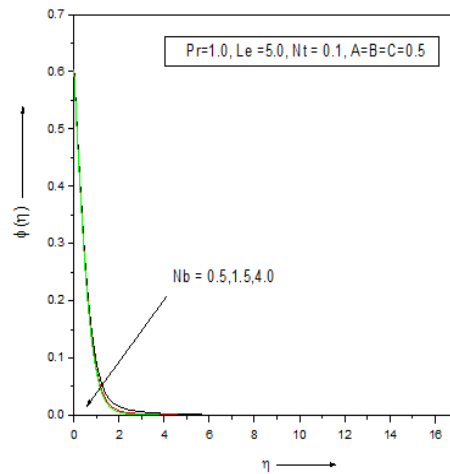


Fig 12. Effects of Brownian motion parameter Nb on the concentration profiles.

V. CONCLUSIONS

In this paper, effects of velocity, thermal and solutal slip boundary conditions on the flow and heat transfer of nanofluids past a linear stretching sheet with prescribed constant wall temperature is investigated. The boundary layer equations governing the flow are reduced to a set of non-linear ordinary differential equations using a similarity transformation. The obtained differential equations are solved numerically by using an efficient fourth order Runge-Kutta method along with Shooting technique has been employed for different combinations of nano fluid parameters (or governing parameters). It has been theoretically analyzed the influence of various governing parameters including Prandtl number (Pr), Lewis number (Le), Brownian motion parameter (Nb), thermophoresis parameter (Nt) velocity slip parameter (A), thermal slip parameter (B) and solutal slip parameter (C) on the momentum, thermal and concentration boundary layer are discussed using tables and figures. The numerical results obtained are in excellent agreement with the previously published data in limiting condition and for some particular cases of the present study.

The main findings of the study are summarized as follows:

- (i) As the value of velocity slip parameter A increases, the normal velocity profile and main stream velocity or lateral velocity $f'(\eta)$ profile decreases where as magnitude of wall shear stress profile increases. Further it is observed that for velocity slip parameter A=0 (i.e. no-slip condition) the graph touch one, hence it satisfies usual boundary condition $f'(0) = 1$. In other words we can say momentum boundary layer thickness decreases as the velocity parameter A increases.
- (ii) As the value of velocity slip parameter A increases the skin friction coefficient $-f''(0)$ decreases, which permits more fluid to slip past the sheet. Any further, increase of slip parameter A results is decrease in magnitude and finally approaches to zero i.e. the flow behaves as though it were inviscid.
- (iii) As the values of velocity slip parameter (A = 0, 0.5, 1, 2, 5) increases the temperature profile (i.e. thermal boundary layer thickness) and concentration profile (i.e. concentration boundary layer thickness) increases respectively. (Which results in thickening of the thermal boundary layer thickness).
- (iv) As the values of thermal slip parameter B increases the temperature profile decreases, which results in thickening of concentration boundary layer where as the values of solutal slip parameter (C = 0, 0.5, 1, 2, 5) increases the concentration profile

decreases, which results in thinning of concentration boundary layer.

(v) Concentration boundary layer thickness increases with an increase in thermophoresis parameter (Nt = 0.1, 0.5, 1, 1.5, 2) but it decreases with an increase in Brownian motion parameter (Nb = 0.5, 1.5, 4.0). The influence of thermophoresis parameter on concentration profile graph is monotonic, i.e. as the values of Nt parameter increase, the concentration boundary layer thickness is also increasing.

(vi) The concentration profile decreases as the values of Lewis number Le increases where as the temperature profile decreases as values of Prandtl number Pr increases. Further, an increase in the Prandtl number means slow rate of thermal diffusion.

(vii) As the value of both the thermophoresis parameter Nt and Brownian motion parameter Nb increases the temperature profile increases, which results in thickening of the thermal boundary layer thickness.

(viii) As the slip parameter A increases Nusselt number decreases and Sherwood number decreases. As the Nt increases Nusselt number decreases and Sherwood number initially decreases afterwards increases as the value of Nt increases.

(ix) As the slip parameter B increases nusselt number decreases and sherwood number increases. As the Nt increases Nusselt number decreases and Sherwood number increases (B=0) and decrease for (B=1,2)

(x) As the slip parameter C increases nusselt number increases and Sherwood number decreases. As the Nt increases nusselt number decreases and Sherwood number initially decreases but increases as the value of Nt increases.

REFERENCES

- [1] Kuznetsov AV, Nield DA. Natural convective boundary-layer flow of a nanofluid past a vertical plate. *Int. J. Therm. Sci.* 2010; **49**: 243-7.
- [2] Khan WA, Pop I. Boundary layer flow of a nanofluid past a stretching sheet. *Int. J. Heat Mass Transfer* 2010; **53**: 2477-83.
- [3] Ibrahim W, Shanker B. Boundary layer flow and heat transfer of a nanofluid over a vertical plate with convective surface boundary condition. *J Fluid Eng-Trans ASME* 2012; **134**. 081203-1.
- [4] Haddad Z, Nada A, Oztop F, Mataoui A. Natural convection in nanofluids are the thermophoresis and Brownian motion effect significant in nanofluids heat transfer enhancement. *Int. J. Therm. Sci.* 2012; **57**: 152-62.
- [5] Bachok N, Ishak A, Pop I. Boundary-layer flow of nanofluids over a moving surface in a following fluid. *Int. J. Therm. Sci.*, 2010; **49**: 1663-8.
- [6] Makinde OD, Aziz A. Boundary layer of a nano fluid past a stretching sheet with convective boundary condition. *Int. J. Therm. Sci.* 2011; **50**: 1326-32.

- [7] Vajravelu K, Prasad K.V., Jinho L, Changhoon L, Pop I, Robert A, et al. Convective heat transfer in the flow of viscous Ag-water and Cu-water nanofluids over a stretching surface. *Int. J. Therm. Sci.* 2011; **50**: 843-51.
- [8] Andersson H. Slip flow past a stretching surface. *Acta Mech.* 2002; **158**: 121-5.
- [9] Wang CY. Flow due to a stretching boundary with partial slip-an exact solution of the Navier-Stokes equation. *Chem. Eng. Sci.* 2002; **57**: 3745-7.
- [10] Wang CY. Stagnation slip flow and heat transfer on a moving plate. *Chem. Eng. Sci.* 2006; **61**: 7668-72.
- [11] Fang T, Zang J, Yao S. Slip MHD viscous flow over a stretching sheet-an exact solution. *Commun Non-linear Sci. Numer. Simul* 2009; **14**: 3731-7.
- [12] P.Donald Ariel. Axisymmetric flow due to a stretching sheet with partial slip. *Computers and Math. with Appl.* **54**(2007)1169-1183.
- [13] T.Hayat, T.Javed, Z.Abbas, Slip flow and heat transfer of a second grade fluid past a stretching sheet through a porous space. *Int. J. Heat Mass Transfer* **51**(2008)4528-4534.
- [14] M. Turkyilmazoglu. Analytic heat and mass transfer of the mixed hydrodynamic/thermal slip MHD viscous flow over a stretching sheet. Manuscript mathematics department University of Hacettepe, 06532- Beytepe, Ankara, Turkey(2010).
- [15] Abdul Aziz. Hydrodynamic and thermal slip flow boundary layers over a flat plate with constant heat flux boundary conditions. *Commun. Non-Linear Sci. Numer. simulate* **15**(2010)573-580.
- [16] Bikash Sahoo, Sebastien Poncet. Flow and heat transfer of a third grade fluid past an exponentially stretching sheet with partial slip boundary condition. *Int. J. Heat Mass Transfer* **54**(2011)5010-5019.
- [17] M.Turkyilmazoglu. Multiple solutions of heat and mass transfer of MHD slip flow for the viscoelastic fluid over a stretching sheet. *Int. J. Therm. Sci.* **xxx** (2011)1-13.
- [18] M.M. Rahman, Locally similar solutions for hydromagnetic and thermal slip flow boundary layers over a flat plate with variable fluid properties and convective surface boundary condition. *Meccanica* (2011)**46**: 1127-1143.
- [19] Bikash Sahoo, Flow and heat transfer of a non-Newtonian fluid past a stretching sheet with partial slip. *Commun Non-linear Sci. Numer. simulat* **15**(2010)602-615.
- [20] Bikash Sahoo, Effects of slip on sheet-driven flow and heat transfer of a non-Newtonian fluid past a stretching sheet. *Com. Math. Appl.* **61**(2011)1442-1456.
- [21] Dileep Singh Chauhan, Amala Olkha, Slip flow and heat transfer of a second grade fluid in a porous medium over a stretching sheet with power-law surface temperature or heat flux. *Chemical Eng. Comm.* (2011) **198**:9,1129-1145.
- [22] Aminreza Noghrehabadi, Rashid Pourrajab, Mohammad Ghalambaz. Effect of partial slip boundary condition on the flow and heat transfer of nanofluids past stretching sheet prescribed constant wall temperature. *Int. J. Therm. Sci.* **54**(2012) 253-261.
- [23] Wubshet Ibrahim, Bandari Shankar. MHD boundary layer flow and heat transfer of a nanofluid past a permeable stretching sheet with velocity, thermal and solutal slip boundary conditions. *Comp. Fluids* **75**(2013)1-10.
- [24] D.A. Nield, A.V. Kuznetsov: The Cheng-Minkowycz problem for natural convective boundary layer flow in a porous medium saturated by a nanofluid, *Int. J. Heat and Mass Transfer* **52**(2009) 5792-5795.
- [25] Hayat T, Qasim M, Mesloub S. MHD flow and heat transfer over permeable stretching sheet with slip conditions. *Int. J. Numer. Meth. Fluid* 2011; **66**: 963-75.